

New Magnetic Resonance Imaging-Based Method for Defining the Extent of Left Atrial Wall Injury After the Ablation of Atrial Fibrillation

Christopher J. McGann, MD,* Eugene G. Kholmowski, PhD,* Robert S. Oakes, BS,†‡
Joshua J. E. Blauer, BS,†‡ Marcos Daccarett, MD,† Nathan Segerson, MD,† Kelly J. Airey, MD,†
Nazem Akoum, MD,† Eric Fish,†‡ Troy J. Badger, MD,† Edward V. R. DiBella, PhD,*‡
Dennis Parker, PhD,*‡ Rob S. MacLeod, PhD,†‡ Nassir F. Marrouche, MD†

Salt Lake City, Utah

Objectives

We describe a noninvasive method of detecting and quantifying left atrial (LA) wall injury after pulmonary vein antrum isolation (PVAI) in patients with atrial fibrillation (AF). Using a 3-dimensional (3D) delayed-enhancement magnetic resonance imaging (MRI) sequence and novel processing methods, LA wall scarring is visualized at high resolution after radiofrequency ablation (RFA).

Background

Radiofrequency ablation to achieve PVAI is a promising approach to curing AF. Controlled lesion delivery and scar formation within the LA are indicators of procedural success, but the assessment of these factors is limited to invasive methods. Noninvasive evaluation of LA wall injury to assess permanent tissue injury may be an important step in improving procedural success.

Methods

Imaging of the LA wall with a 3D delayed-enhanced cardiac MRI sequence was performed before and 3 months after ablation in 46 patients undergoing PVAI for AF. Our 3D respiratory-navigated MRI sequence using parallel imaging resulted in $1.25 \times 1.25 \times 2.5$ mm (reconstructed to $0.6 \times 0.6 \times 1.25$ mm) spatial resolution with imaging times ranging 8 to 12 min.

Results

Radiofrequency ablation resulted in hyperenhancement of the LA wall in all patients post-PVAI and may represent tissue scarring. New methods of reconstructing the LA in 3D allowed quantification of LA scarring using automated methods. Arrhythmia recurrence at 3 months correlated with the degree of wall enhancement with $>13\%$ injury predicting freedom from AF (odds ratio: 18.5, 95% confidence interval: 1.27 to 268, $p = 0.032$).

Conclusions

We define noninvasive MRI methods that allow for the detection and quantification of LA wall scarring after RF ablation in patients with AF. Moreover, there seems to be a correlation between the extent of LA wall injury and short-term procedural outcome. (J Am Coll Cardiol 2008;52:1263–71) © 2008 by the American College of Cardiology Foundation

Atrial fibrillation (AF) is a growing clinical problem with enormous impact on both short-term quality of life and long-term survival (1,2). Radiofrequency ablation (RFA) targeting the pulmonary veins' ostia and antra has been proven to be effective in managing patients with AF (3–5). Controlled lesion delivery and scar formation within the left atrium (LA) are indicators of procedural success, but the assessment of these factors is limited to invasive methods

(6). As a result, a noninvasive evaluation of LA wall injury to assess permanent tissue injury may be an important step in improving procedural success.

See page 1272

Delayed-enhancement cardiovascular magnetic resonance imaging (DE-CMRI) is an established noninvasive clinical method for characterizing tissue in a variety of cardiac disease processes, including after myocardial infarction and injury due to myocarditis (7–14). Contrast enhancement in injured tissue using magnetic resonance imaging (MRI) occurs because of altered washout kinetics of gadolinium relative to the normal surrounding tissue. Magnetic reso-

From the *Radiology Department and the †Division of Cardiology, Internal Medicine, University of Utah School of Medicine, and the ‡Bioengineering Department, University of Utah, Salt Lake City, Utah. Drs. Dibella, Parker, and Kholmowski are partially supported by grants from Siemens Medical Corporation.

Manuscript received February 22, 2008; revised manuscript received April 11, 2008, accepted May 5, 2008.

Abbreviations and Acronyms

3D	= three-dimensional
AF	= atrial fibrillation
CI	= confidence interval
DE-CMRI	= delayed-enhancement cardiac magnetic resonance imaging
ECG	= electrocardiogram
FLASH	= fast low angle shot
GRAPPA	= generalized autocalibrating partially parallel acquisitions
LA	= left atrium/atrial
LV	= left ventricle/ventricular
MRI	= magnetic resonance imaging
OR	= odds ratio
PVAI	= pulmonary vein antrum isolation
RFA	= radiofrequency ablation
RF	= radiofrequency
TE	= echo time
TI	= inversion time
TR	= repetition time

nance imaging has been successfully used to detect tissue injury caused by radiofrequency (RF) lesion formation, although data are limited. Animal studies have shown acute RF lesions in the right ventricle in dogs as a result of heat-related changes in T1 and T2 parameters in the necrotic myocardium (15). Formation of RF lesions on the epicardium of dogs also has been characterized in several phases up to 12 h after injury using gadolinium-enhanced MRI and right ventricular enhancement correlated with histopathology showing coagulation necrosis with loss of cellular and vascular architecture (16). In humans, Peters et al. (17) reported on their initial experience using 3-dimensional (3D) DE-CMRI to detect LA scar 1 to 3 months after AF ablation, and a case of left ventricular (LV) injury from previous RF ablation in a patient treated for idiopathic LV tachycardia also has been reported (18).

Although these data suggest that MRI is well suited to provide important noninvasive evaluation of RFA lesions, human studies are lacking and its clinical role is still undefined. This study sought to detect and evaluate LA wall injury in patients with AF after PVAI using novel MRI methods and image processing. Results discussed here may help better define procedure outcome, guide follow-up treatment, and develop strategies to avoid complications.

Methods

Patients. Fifty-three patients referred to the University of Utah for PVAI between December 2006 and July 2007 were enrolled in this study. The protocol was approved by the Institutional Review Board at the University of Utah and was compliant with the Health Insurance Portability and Accountability Act of 1996. After informed consent was obtained, patients underwent pre-PVAI MRI scanning to define the PVs, location of the esophagus, LA anatomy, and characterization of the LA wall tissue. The MRI was repeated 3 months after ablation in all patients.

After the procedure, patients continued anticoagulation therapy with warfarin to maintain an international normalized ratio of 2.0 to 3.0 for a minimum of 3 months. Patients were assessed after 3 months to determine the success of the ablation procedure. Success was defined as a lack of late AF

recurrence while off antiarrhythmic medications. Event monitors were placed for a minimum of 2 months after their PVAI. Patients were instructed to activate the monitors any time they felt symptomatic. To confirm the absence of asymptomatic AF, all patients received a 48-h Holter electrocardiogram (ECG) recording at the 3-month follow-up. Recurrences were determined from patient reporting, event monitoring, Holter monitoring, and ECG data. Recurrent AF was defined as a symptomatic or asymptomatic detected episode lasting >15 s.

Pulmonary vein isolation procedure. The PVAI under intracardiac echocardiogram guidance was performed. A 10-F, 64-element, phased-array ultrasound catheter (AcuNav, Siemens, Mountain View, California) was used to visualize the interatrial septum and to guide the transseptal puncture. A circular mapping catheter (Lasso, BioSense Webster, Diamond Bar, Colorado) and an ablation catheter were inserted into the LA. An intracardiac echocardiogram was used to define the PV ostia and their antra and to help position the circular mapping catheter and ablation catheter at the desired sites. Temperature and power were set to 50° and 50 W (pump flow rate at 30 ml/min), respectively. The RF delivery was interrupted in the case of impedance increase or if a sudden increase in microbubble density was observed during ablation. All study patients underwent PVAI (19) in addition to LA posterior wall and septal debulking.

Delayed-enhancement MRI acquisition sequence. All participants underwent MRI studies on a 1.5-T Avanto clinical scanner (Siemens Medical Solutions, Erlangen, Germany) using a phased-array receiver coil 24 to 72 h before PVAI. The protocol included sequences to define the anatomy of the LA and pulmonary veins. The anatomy was evaluated using the contrast-enhanced 3D fast low angle shot (FLASH) sequence and the cine true-fast imaging with steady state precession sequence. Typical acquisition parameters for 3D FLASH scan were: breath-hold in expiration, a transverse (axial) imaging volume with voxel size = 1.25 × 1.25 × 2.5 mm, repetition time (TR) = 3.1 ms, echo time (TE) = 1.0 ms, and parallel imaging using the generalized autocalibrating partially parallel acquisitions (GRAPPA) technique with reduction factor R = 2 and 32 reference lines, scan time = 14 s. The 3D FLASH scan was acquired twice: pre-contrast and during a first pass of contrast agent (Multihance, Bracco Diagnostic Inc., Princeton, New Jersey), intravenous injection of a dose of 0.1 mmol/kg body weight, 2-ml/s injection rate, followed by a 15-ml saline flush). Timing of the first pass scan was defined using a MRI fluoroscopic scan.

Complete coverage of the LA was achieved with 16 to 22 transverse 2-dimensional slices acquired during retrospective ECG-gated, cine pulse sequence. All of the images were acquired during breath-hold in expiration (1 or 2 slices per breath-hold depending on the subject heart rate and tolerance to breath-holding) and were used to evaluate the LA morphology during the cardiac cycle. Typical scan

parameters were: 6-mm slice thickness, no gap between slices, pixel size = 2.0×2.0 mm, TR/TE = 2.56/1.03 ms, GRAPPA with R = 2 and 44 reference lines, 15 views/segment.

Delayed enhancement MRI was used to identify fibrous tissue in the LA. The DE-CMRI was acquired 15 min after the contrast agent injection using a 3D inversion recovery-prepared, respiration-navigated, ECG-gated, gradient echo pulse sequence. Typical acquisition parameters were as follows: free breathing using navigator gating, a transverse imaging volume with voxel size = $1.25 \times 1.25 \times 2.5$ mm (reconstructed to $0.625 \times 0.625 \times 1.25$ mm), TR/TE = 6.3/2.3 ms, inversion time (TI) = 230 to 270 ms, and GRAPPA with R = 2 and 32 reference lines. Electrocardiogram gating was used to acquire a small subset of phase-encoding views used during the diastolic phase of the LA cardiac cycle. The time interval between the R-peak of the ECG and the start of data acquisition was defined using the cine images of the LA. Fat saturation was used to suppress the fat signal. The TE of the scan (2.3 ms) was chosen so that fat and water are out of phase and the signal intensity of partial volume fat-tissue voxels was reduced, which allowed for improved delineation of the LA wall boundary. The TI value for the DE-CMRI scan was identified using a scout scan. Typical scan time for the DE-CMRI study was 5 to 10 min depending on subject respiration and heart rate. If the first acquisition did not have an optimal TI or had substantial motion artifacts, the scan was repeated.

Image processing and analysis. All MR images were evaluated and interpreted by 2 independent operators experienced in CMRI. Processing of the MRI digital imaging and communications in medicine (DICOM) formatted data sets were performed using OsiriX (open-source) for visualization, whereas quantification of images was performed using Matlab (Mathworks, Inc., Natick, Massachusetts). The LA data from 3D DE-CMRI acquisitions were evaluated slice by slice and using volume rendering tools. These images were segmented and rendered, which allowed for unique visualization of LA wall RF injury patterns using the entire data set and facilitated correlation with 3D CARTO images. Visualization was performed using smooth table opacity.

In patients who underwent post-procedural MRI scans, the relative extent of injury within the volume was measured using a threshold-based lesion detection algorithm. In all images, the epicardial and endocardial borders were manually contoured using custom image display and analysis software written in Matlab. Care was made in 2-dimensional tracings of the endocardial and epicardial walls to confine the region of interest to only the LA wall and to avoid the blood pool, particularly on the right side, where a navigator-induced artifact was present in some patient scans. Normal and injured tissue were defined based on a bimodal distribution of pixel intensities within the LA wall. The first mode of lower pixel intensities was chosen as normal tissue. Injured

tissue was defined at 3 standard deviations above the normal tissue mean pixel intensity. Regions defined as lesion were visualized independently to ensure appropriateness of lesion detection. The LA lesion area for each slice was summed for the entire scan and reported as a ratio of lesion volume to total LA wall volume. For selected patients with characteristic patterns of lesion formation observed in the OsiriX 3D visualizations, image masks of injured regions were reconstructed into 3D volumes for comparison with the OsiriX visualizations. The investigators were blinded during the analysis of all imaging and electrophysiology data.

Follow-up. All patients were monitored overnight on a telemetry unit after the procedure. Warfarin (INR 2 to 3) was restarted in all patients the day of PVAI, and was continued for a minimum of 3 months in paroxysmal and for 6 months in persistent and permanent AF patients. Patients were followed up in the outpatient clinic 3 months post-ablation, at which point they underwent an MRI scan to assess for PV stenosis, degree of chronic LA scarring, and Holter monitor recording for 24 to 48 h.

Statistical methods. Normal continuous variables are presented as mean \pm SD. Continuous data were analyzed by the Student *t* test to test for significant differences. Chi-square tests were used to test for differences in categorical measurements. Differences were considered significant at $p < 0.05$. Statistical analysis was performed using the SPSS 15.0 statistical package (SPSS Inc., Chicago, Illinois).

Table 1 Patient Demographics, Summary by Response to Procedure

	Responders (n = 35)	Nonresponders (n = 11)	p Value*
Type of atrial fibrillation			0.118
Paroxysmal	19 (54.3%)	3 (27.3%)	
Persistent	16 (45.7%)	8 (72.7%)	
Gender			
Female	12 (34.3%)	5 (45.5%)	0.503
Male	23 (65.7%)	6 (54.5%)	
Hypertension	18 (2.9%)	3 (27.3%)	0.161
Diabetes	5 (14.3%)	—	0.184
Coronary artery disease	4 (11.4%)	2 (18.2%)	0.562
History of smoking	5 (17.1%)	4 (36.4%)	0.107
Valve surgery	1 (2.8%)	—	0.571
Myocardial infarction	2 (5.7%)	1 (9.1%)	0.692
Mitral stenosis	4 (11.4%)	—	0.241
Age (yrs)	63.1 \pm 11.9	71.4 \pm 11.4	0.048
Left ventricular ejection fraction (%)	57.1 \pm 4.9	49.5 \pm 9.6	0.002
Left atrial area, pre-PVAI (cm ²)	20.1 \pm 8.5	24.9 \pm 6.4	0.147
Left atrial volume, pre-PVAI (cm ³)	84.8 \pm 24.5	128.3 \pm 29.8	<0.001
Antiarrhythmic medications			
None	19 (54.3%)	7 (63.6%)	0.567
One medication	12 (34.3%)	2 (18.2%)	
Multiple medications	4 (11.4%)	2 (18.2%)	

PVAI = pulmonary vein antrum isolation.

Results

Patients. Fifty-three patients who underwent PVAI for treatment of AF during the study period and completed the MRI scanning protocol were included in the analysis. Seven of the 53 patients were excluded because of inadequate MR images. The patients removed included 6 with poor image quality on the pre- or post-ablation scans and 1 who received an insufficient dose of intravenous contrast. Poor image quality resulted from patient motion and significant cardiac arrhythmia. In 1 case, navigator signal interference precluded accurate analysis. Results from the remaining 46 patients were included in the data.

Table 1 shows the patient demographics for responders and nonresponders to PVAI treatment. Statistically signif-

icant differences were seen among the study populations for age, LV ejection fraction, LA area, and LA volume and are consistent with prior published data (20–34).

DE-CMRI visualization and quantification. Hyperenhancement in the left atrium was not seen in patients at baseline prior to the ablation. Mild signal in the LA wall was seen in 4 patient scans (8.7%); however, it was clearly lower intensity than scans post-ablation injury. In addition, the pre-ablation enhancement did not meet the threshold for hyperenhancement determined by our quantification algorithm, which was modeled after previously published methods (35,36). Clear contrast enhancement was seen in all (46 of 46, 100%) of the post-ablation images, most commonly in the posterior LA wall, interatrial septum, and surrounding the

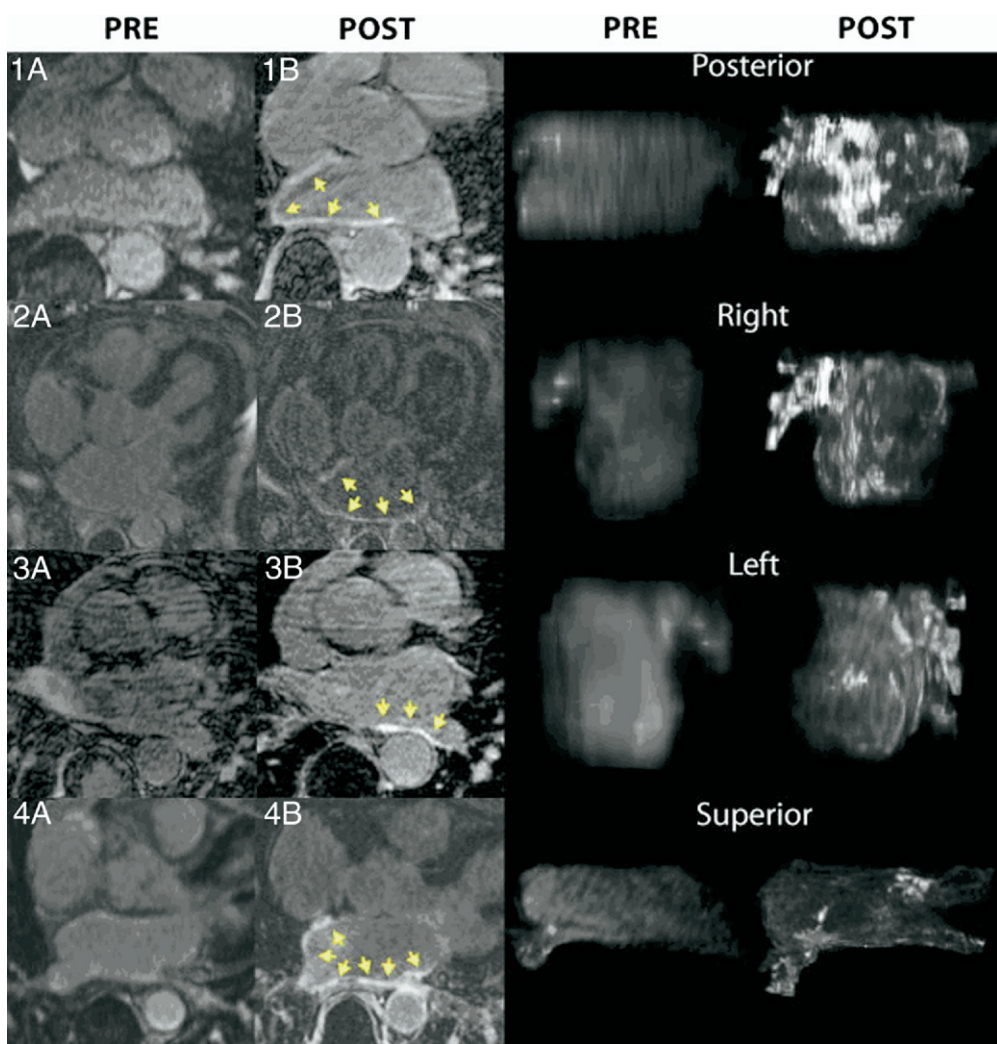


Figure 1 Left Atrial Injury Before PVAI and 3 Months After PVAI on 3D DE-CMRI

Left panels show LA wall slices at baseline (**A**) and 3 months after PVAI (**B**) on 3D navigated DE-CMRI in 4 different patients. **Right panels** show 3D rendering of LA in Patient #1 before and after PVAI in multiple views (posterior, right, left, and superior) reconstructed from MRI slice data. Post-PVAI hyperenhancement of LA wall is clearly seen (**yellow arrows**) in regions subjected to RF ablation and suggests scarring. 3D = three-dimensional; DE-CMRI = delayed-enhancement cardiac magnetic resonance imaging; LA = left atrial/atrium; MRI = magnetic resonance imaging; PVAI = pulmonary vein antrum isolation; RF = radiofrequency.

pulmonary veins (Fig. 1). Two experienced independent operators evaluated the presence or absence of contrast enhancement on DE-CMRI with agreement in all cases. Enhancement within the right pulmonary veins occurred in some patients. This was caused by the navigator RF pulse located over the right hemidiaphragm and did not reflect tissue injury. This navigator-induced interference was differentiated from enhancement by its location and intensity. A recent change made to the pulse sequence has resulted in a complete removal of the navigator interference (data not shown).

Figure 1 shows MRI slices for 4 separate patients at baseline and 3 months after PVAI. As noted, the injury to the LA wall is largely located in the posterior wall, PV ostia, and interatrial septum. However, degree of injury varied greatly among patients. The anterior LA wall was consistently spared and free of MRI evidence of injury in all patients, which is consistent with current strategies for catheter ablation of AF. Figure 1 also shows an example of 3D visualization of the LA wall in Patient #1 before and after ablation in 4 different orientations: posterior, right, left, and superior views.

Figure 2 shows LA injury detection using the semiautomated computer algorithm. When injury as identified by the computer algorithm is overlaid with 3D visualization, there is a strong correlation between the observed injury patterns and the region identified as scar by the algorithm. Figure 3 shows the overlay for 1 patient in 3 dimensions. An LA injury identified by the computer algorithm (blue) matches regions of hyperenhancement (white) in the MRI visualization. Similar correlation

between MRI visualization and algorithm detection were seen for all patients. This segmentation algorithm in conjunction with the DE-CMRI data allowed LA wall injury to be quantified as a percentage of the total LA wall volume.

Quantification of LA wall injury and patient outcome. At 3 months, 35 of 46 patients (76.1%) remained free of AF recurrence. All who suffered AF recurrences were placed back on antiarrhythmic drugs. Although a higher percentage of individuals who did not respond to therapy and suffered recurrence had persistent/permanent AF (8 of 11, 72.7%) versus those who responded to therapy (16 of 35, 45.7%), this difference failed to reach statistical significance ($p = 0.118$).

A large difference was seen between the percentage of LA wall injury (as determined by MRI and semiautomated quantification) between responders and nonresponders to PVAI (Fig. 4). In patients who responded to ablation, the average LA wall injury was $19.3 \pm 6.7\%$, whereas in those who did not respond, the average LA wall injury was $12.4 \pm 5.7\%$ ($p = 0.004$). The strong association between average LA wall injury and recurrence persisted when stratifying patients by the first and second quartiles. Using the first quartile (LA wall injury $> 13\%$), patients with large scars were $18.5 \times$ less likely to suffer recurrence of AF (odds ratio [OR]: 18.5, 95% confidence interval [CI]: 1.27 to 268, $p = 0.032$). After controlling for age, gender, ablation time, and type of AF, large scar areas strongly predicted the absence of recurrences (adjusted OR: 83.7, 95% CI: 2.013 to 3,481.1, $p = 0.022$).

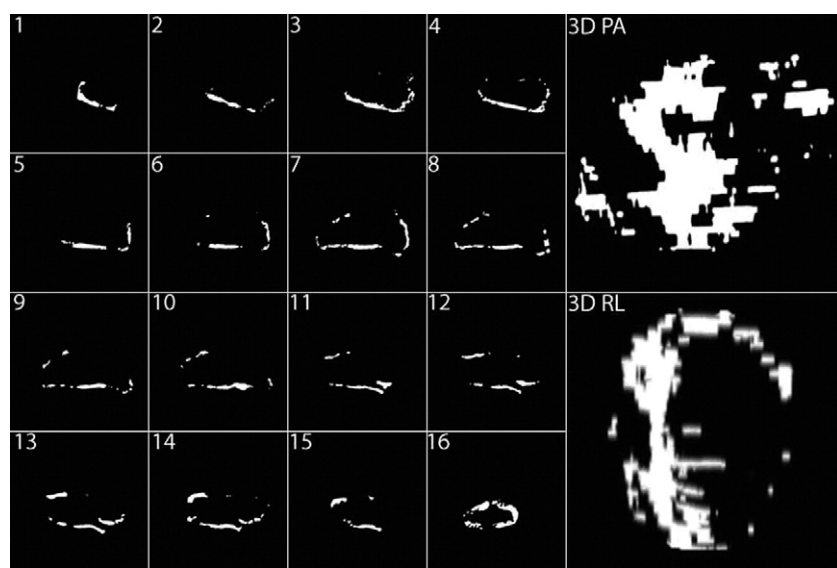


Figure 2 **Automated Quantification of Chronic LA Injury 3 Months After PVAI**

Left atrial wall injury was determined using a threshold based on the defined normal wall regions. **Panels 1 to 16** show extent of injury at 5 standard deviations in a subset of slices from the 3D DE-CMRI from Patient #1 (Fig. 1). Reconstruction in 3D of the full set of data is shown in the **right panels** (3D PA and RL views). Using these methods, LA injury volume can be determined and calculated as a percentage of total LA wall volume. PA = posterior-anterior; RL = right-left; other abbreviations as in Figure 1.

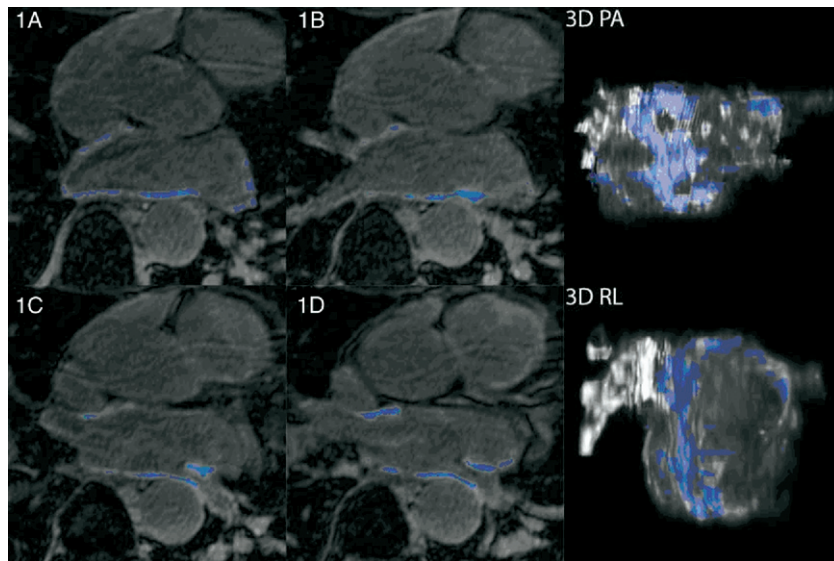


Figure 3 Overlay Images of LA Wall Injury

Panels **1A** to **1D** are 4 example LA slices from the 3D DE-CMRI from Patient #1 (Fig. 1) that show close correlation of LA injury as determined by automated methods using a 3-SD cutoff value (blue transparency) overlaying MRI. **Right panels** show 3D overlay of full data set (3D PA and RL). LA injury mask (**blue**) determined by automated methods should match and overlay hyperenhanced areas (**white**) of true injury on DE-CMRI. Although the left pulmonary veins are white on MRI, this enhancement is attributable to navigator interference, not injured tissue, as we position the navigator over the right hemidiaphragm. The PVs are shown here only to help with anatomical orientation and are excluded from raw data used to produce injury mask by automated methods. Abbreviations as in Figures 1 and 2.

Using the second quartile (median) as the cutoff for large scar areas, the protective association between large scar areas and recurrences was smaller but still persisted ($p = 0.045$).

Discussion

Main findings. In this study, we show LA injury after PVAI visualized by 3D DE-CMRI at high resolution using our novel imaging approach and processing methods. Left atrial wall injury resulting from RF ablation 3 months after PVAI was seen in every patient with a tissue injury pattern

reflecting location of RF energy delivery sites. In addition, injury on MRI seems to reflect tissue scarring, and the degree of scarring correlates with procedural outcomes.

DE-CMRI detects tissue injury from RFA. In patients with ischemic cardiomyopathy, DE-CMRI is used routinely to accurately detect and size infarcted myocardium. It is arguably the gold standard viability study and accurately predicts hibernating myocardium and response to revascularization (37,38). Performing DE-CMRI to detect LA wall injury is challenging as the LA is a thin wall structure

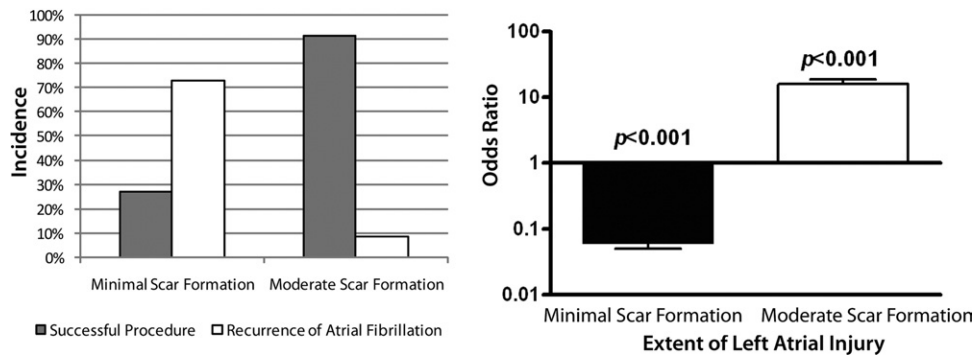


Figure 4 Association Between Atrial Fibrillation Recurrences and Clinical Success According to LA Wall Injury After Catheter-Based PVAI

Patients with minimal scar formation at 3 months after the procedure ($>13\%$ of LA myocardial volume enhancement on DE-MRI) had low procedural success and a high recurrence of atrial fibrillation, whereas patients with moderate scar formation at 3 months had very high procedural success and a low recurrence of atrial fibrillation. Abbreviations as in Figure 1.

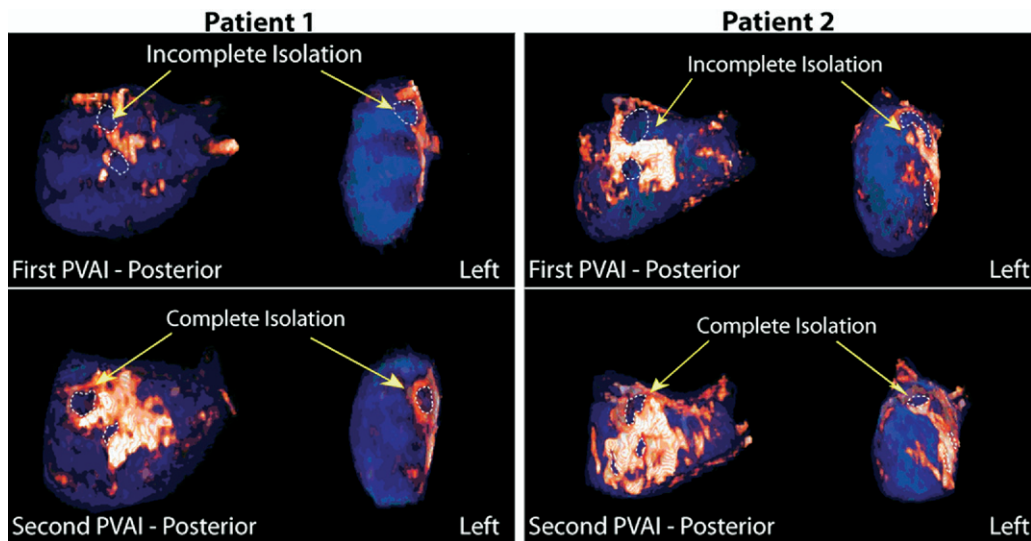


Figure 5 Delayed-Enhancement MRI Scans Acquired 3 Months After a First (Failed) Procedure and a Second (Successful) Procedure

Incomplete scar formation located near the antrum of the pulmonary veins after failed isolation was noted in both patient examples. The gap in RF lesions at the pulmonary vein antrum (**purple**) correlated with incomplete electrical isolation of the left superior pulmonary vein. Delayed-enhancement MRI at 3 months after the repeat PVAI shows complete scar formation (**white/orange**) isolating the pulmonary veins. Both patients were free of AF at follow-up. Posterior and left lateral views are shown. Abbreviations as in Figure 1.

compared with the LV, and thus requires better spatial resolution while maintaining adequate contrast-to-noise ratio and signal-to-noise ratio. The MRI pulse sequence we use is a 3D high-resolution sequence similar to one reported on by Peters et al. (17) and achieves spatial resolution much greater than that typical for 2D delayed enhancement used in LV viability studies. In addition, we were able to take advantage of parallel imaging to significantly reduce the scan time and, as a result, reduce motion artifact.

Processing enhancements here greatly facilitated a more comprehensive evaluation of LA wall injury from images acquired from MRI images. Using a DICOM image editor, we developed methods to view the entire LA wall injury volume rendered in 3D from the slice data set, which facilitated comparisons with other important 3D image data, including CARTO-derived voltage maps, sites of RF energy deposition, and the LA angiogram. Visualization of LA wall injury in 3D also improved assessment of lesion confluence and atrial debulking resulting from PVAI.

Injury patterns on DE-CMRI and tissue scarring in the LA. Effective injury to the LA wall and permanent tissue injury are important for procedural success (39). Although invasive electroanatomical mapping is an important tool to help establish tissue ablation during the procedure, lesion recovery and incomplete sampling limit accurate and comprehensive assessment of permanent tissue injury. Noninvasive detection of LA wall injury using DE-CMRI is a recent advancement that reliably detected injury at 3 months in all of our patients (46 of 46 patients, no interobserver

variability). In addition, the entire LA wall is visualized on 3D MRI and serial evaluation is safe and noninvasive.

There are a number of potential applications of our visualization technique and analysis. One such technique would analyze potential reasons for AF recurrence, such as that when loss of electrical isolation after PVAI has occurred (40). Visualization of the pulmonary veins and LA using 3D image processing allows for the scar pattern to be assessed and subsequent isolation procedures to be planned. Figure 5 shows visualizations of DE-MRI scans of 2 patients acquired 3 months after a failed PVAI.

These patients elected to undergo a second ablation procedure and had a second DE-MRI scan acquired after that procedure. Three-dimensional segmentation of the LA was performed according to the methods described. Incomplete scar formation can be seen near the antrum of the pulmonary veins after the failed PVAI procedure. This gap in RF lesions at the pulmonary vein antrum (purple) correlated with incomplete electrical isolation of the left superior vein (as determined by electrophysiology study at the time of the second procedure). After the repeat procedure, the MRI shows complete scar formation around the ostia of the left superior vein (Figs. 1C, 1D, 2C, 2D, and 5) in both patients. Three months after the second procedure, both patients were free of AF (as determined by 8-day Holter recordings and patient self-report). In such an application, 3D processing provides an advantage over traditional 2D visualization because it allows for the spatial relationships and complex geometry of the LA to be better

Table 2 Patients at 3-Month Follow-Up

	Responders (n = 35)	Nonresponders (n = 11)	p Value*
Percent LA wall injury	19.3 ± 6.7	12.4 ± 5.7	0.004
Degree of scar formation			
Minimal scar formation (>13% of volume enhancement)	3 (8.6%)	8 (72.7%)	<0.001
Moderate scar formation (<13% of left atrial volume)	32 (91.4%)	3 (27.3%)	<0.001
LA area (cm ²), 3-month follow-up	18.0 ± 5.0	24.4 ± 4.6	<0.001
LA volume (cm ³), 3-month follow-up	74.1 ± 26.4	110.3 ± 16.8	<0.001

LA = left atrial.

appreciated. This will likely lead to improved procedure planning and a lower recurrence rate of AF.

LA wall injury on MRI predicted procedural outcome. Although all patients in this study had detectable injury on 3D DE-CMRI 3 months after ablation, the extent of injury varied significantly. When we applied our automated algorithm to quantify LA wall injury, degree of injury was significantly different between responders and nonresponders (Table 2). After controlling for age, gender, AF phenotype, LA size, and LA volume, patients with scar ratios >13% are 18.5 times more likely to have a favorable outcome and freedom from AF at 3 months (OR: 18.5, 95% CI: 1.27 to 268, p = 0.032). These data suggest that degree of LA wall scarring predicts procedural success. Our findings validate preliminary reports that seem to show that procedural outcome correlates with overall enhancement (41).

The overall degree of scar may have important implications to the lesion type and subsequent interruption of PV to LA conduction. Interruption of PV to LA conduction has been an important component of procedural success. Verma et al. (40) reported recurrent AF after PVAI in patients with more PV-to-LA conduction and shorter LA-to-PV delays. In comparison, the majority of patients maintaining sinus rhythm off antiarrhythmic drugs showed no recurrent PV-to-LA conduction and significantly longer LA-to-PV delay. These results are supported by an earlier study by Ouyang et al. (42) showing recovery of PV conduction in patients with recurrent atrial tachyarrhythmias after PVAI. Closing the conduction gaps on repeat procedure later successfully eliminated the arrhythmias. These data suggest that overall lesion permanence and complete PV isolation may be important procedural goals. The findings we present here also seem complimentary to this previous work and may indicate that degree of scarring on DE-CMRI may represent a noninvasive manner of estimating the atrial lesion type and the subsequent electrical isolation (40,42–44).

Study limitations. Although the outcomes data in this study were statistically significant, the sample size was relatively small. In addition, 3D MRI in this study was performed on a 1.5-T scanner. Significant improvements in LA wall imaging with greater spatial resolution, signal-to-

noise ratio, and contrast-to-noise ratio is expected at higher magnetic field (3-T). Although we found that the degree of atrial enhancement (and presumably scar) and freedom from recurrence were linked, we were not able to show whether this was caused by complete and successful isolation at 3 months or simply caused by the destruction of electrically viable tissue to such an extent that the atrium could no longer sustain AF. The standard ablation procedure at our facility incorporates both of these techniques, and as a result, we were unable to differentiate the relative contributions. Prospective studies designed to pursue this question should be conducted.

Conclusions

Noninvasive imaging of the LA wall with MRI is a recent advancement and a powerful tool to evaluate injury related to RF energy delivery during AF ablation. Results reported in our study suggest that the degree of LA wall injury predicts procedural outcome at 3 months.

Reprint requests and correspondence: Dr. Nassir F. Marrouche, Atrial Fibrillation Program and Electrophysiology Laboratory, Division of Cardiology, University of Utah Health Sciences Center, 30 North 1900 East, Room 4A100, Salt Lake City, Utah 84132-2400. E-mail: nassir.marrouche@hsc.utah.edu.

REFERENCES

- Benjamin EJ, Wolf PA, D'Agostino RB, Silbershatz H, Kannel WB, Levy D. Impact of atrial fibrillation on the risk of death: the Framingham Heart Study. *Circulation* 1998;98:946–52.
- Dries DL, Exner DV, Gersh BJ, et al. Atrial fibrillation is associated with an increased risk for mortality and heart failure progression. *J Am Coll Cardiol* 1998;32:695–703.
- Marrouche NF, Dresing T, Cole C, et al. Circular mapping and ablation of the pulmonary vein for treatment of atrial fibrillation: impact of different catheter technologies. *J Am Coll Cardiol* 2002;40:464–74.
- Marrouche NF, Martin DO, Wazni O, et al. Phased-array intracardiac echocardiography monitoring during pulmonary vein isolation in patients with atrial fibrillation: impact on outcome and complications. *Circulation* 2003;107:2710–6.
- Häissaguerre M, Jaïs P, Shah DC, et al. Spontaneous initiation of atrial fibrillation by ectopic beats originating in the pulmonary veins. *N Engl J Med* 1998;339:659–66.
- Oh S, Kilicaslan F, Zhang Y, et al. Avoiding microbubbles formation during radiofrequency left atrial ablation versus continuous microbubbles formation and standard radiofrequency ablation protocols: comparison of energy profiles and chronic lesion characteristics. *J Cardiovasc Electrophysiol* 2006;17:72–7.
- Kim RJ, Fieno DS, Parrish TB, et al. Relationship of MRI delayed contrast enhancement to irreversible injury, infarct age, and contractile function. *Circulation* 1999;100:1992–2002.
- Klein C, Nekolla SG, Bengel FM, et al. Assessment of myocardial viability with contrast-enhanced magnetic resonance imaging: comparison with positron emission tomography. *Circulation* 2002;105:162–7.
- Kim RJ, Wu E, Rafael A, et al. The use of contrast-enhanced magnetic resonance imaging to identify reversible myocardial dysfunction. *N Engl J Med* 2000;343:1445–53.
- De Cobelli F, Pieroni M, Esposito A, et al. Delayed gadolinium-enhanced cardiac magnetic resonance in patients with chronic myocarditis presenting with heart failure or recurrent arrhythmias. *J Am Coll Cardiol* 2006;47:1649–54.

11. Rochitte CE, Tassi EM, Shiozaki AA. The emerging role of MRI in the diagnosis and management of cardiomyopathies. *Curr Cardiol Rep* 2006;8:44–52.
12. Laijs JP, Hyafil F, Feldman LJ, et al. Differentiating acute myocardial infarction from myocarditis: diagnostic value of early- and delayed-perfusion cardiac MR imaging. *Radiology* 2005;237:75–82.
13. Oshinski JN, Han HC, Ku DN, Pettigrew RI. Quantitative prediction of improvement in cardiac function after revascularization with MR imaging and modeling: initial results. *Radiology* 2001;221:515–22.
14. Mahrholdt H, Goedelke C, Wagner A, et al. Cardiovascular magnetic resonance assessment of human myocarditis: a comparison to histology and molecular pathology. *Circulation* 2004;109:1250–8.
15. Lardo AC, McVeigh ER, Jumrusrikul P, et al. Visualization and temporal/spatial characterization of cardiac radiofrequency ablation lesions using magnetic resonance imaging. *Circulation* 2000;102:698–705.
16. Dickfeld T, Kato R, Zviman M, et al. Characterization of radiofrequency ablation lesions with gadolinium-enhanced cardiovascular magnetic resonance imaging. *J Am Coll Cardiol* 2006;47:370–8.
17. Peters DC, Wylie JV, Hauser TH, et al. Detection of pulmonary vein and left atrial scar after catheter ablation with three-dimensional navigator-gated delayed enhancement MR imaging: initial experience. *Radiology* 2007;243:690–5.
18. Sievers B, Brandts B, Moon JC, Pennell DJ, Trappe HJ. Cardiovascular magnetic resonance of iatrogenic ventricular scarring due to catheter ablation for left ventricular tachycardia. *Int J Cardiol* 2003;91:249–50.
19. Kanj MH, Wazni O, Fahmy T, et al. Pulmonary vein antral isolation using an open irrigation ablation catheter for the treatment of atrial fibrillation: a randomized pilot study. *J Am Coll Cardiol* 2007;49:1634–41.
20. Pritchett AM, Jacobsen SJ, Mahoney DW, et al. Left atrial volume as an index of left atrial size: a population-based study. *J Am Coll Cardiol* 2003;41:1036–43.
21. Natale A, Newby KH, Pisano E, et al. Prospective randomized comparison of antiarrhythmic therapy versus first-line radiofrequency ablation in patients with atrial flutter. *J Am Coll Cardiol* 2000;35:1898–904.
22. Wazni OM, Marrouche NF, Martin DO, et al. Radiofrequency ablation vs antiarrhythmic drugs as first-line treatment of symptomatic atrial fibrillation: a randomized trial. *JAMA* 2005;293:2634–40.
23. Karch MR, Zrenner B, Deisenhofer I, et al. Freedom from atrial tachyarrhythmias after catheter ablation of atrial fibrillation: a randomized comparison between 2 current ablation strategies. *Circulation* 2005;111:2875–80.
24. Oral H, Pappone C, Chugh A, et al. Circumferential pulmonary-vein ablation for chronic atrial fibrillation. *N Engl J Med* 2006;354:934–41.
25. Gaita F, Riccardi R, Caponi D, et al. Linear cryoablation of the left atrium versus pulmonary vein cryoisolation in patients with permanent atrial fibrillation and valvular heart disease: correlation of electroanatomic mapping and long-term clinical results. *Circulation* 2005;111:136–42.
26. Haïssaguerre M, Hocini M, Sanders P, et al. Catheter ablation of long-lasting persistent atrial fibrillation: clinical outcome and mechanisms of subsequent arrhythmias. *J Cardiovasc Electrophysiol* 2005;16:1138–47.
27. Sanders P, Morton JB, Davidson NC, et al. Electrical remodeling of the atria in congestive heart failure: electrophysiological and electro-anatomic mapping in humans. *Circulation* 2003;108:1461–8.
28. Nademanee K, McKenzie J, Kosar E, et al. A new approach for catheter ablation of atrial fibrillation: mapping of the electrophysiologic substrate. *J Am Coll Cardiol* 2004;43:2044–53.
29. Haïssaguerre M, Sanders P, Hocini M, et al. Catheter ablation of long-lasting persistent atrial fibrillation: critical structures for termination. *J Cardiovasc Electrophysiol* 2005;16:1125–37.
30. Willems S, Klemm H, Rostock T, et al. Substrate modification combined with pulmonary vein isolation improves outcome of catheter ablation in patients with persistent atrial fibrillation: a prospective randomized comparison. *Eur Heart J* 2006;27:2871–8.
31. Calo L, Lamberti F, Loricchio ML, et al. Left atrial ablation versus biatrial ablation for persistent and permanent atrial fibrillation: a prospective and randomized study. *J Am Coll Cardiol* 2006;47:2504–12.
32. Kistler PM, Rajappan K, Jahngir M, et al. The impact of CT image integration into an electroanatomic mapping system on clinical outcomes of catheter ablation of atrial fibrillation. *J Cardiovasc Electrophysiol* 2006;17:1093–101.
33. Sauer WH, McKernan ML, Lin D, Gerstenfeld EP, Callans DJ, Marchlinski FE. Clinical predictors and outcomes associated with acute return of pulmonary vein conduction during pulmonary vein isolation for treatment of atrial fibrillation. *Heart Rhythm* 2006;3:1024–8.
34. Chugh A, Oral H, Lemola K, et al. Prevalence, mechanisms, and clinical significance of macroreentrant atrial tachycardia during and following left atrial ablation for atrial fibrillation. *Heart Rhythm* 2005;2:464–71.
35. Hsu LY, Natanzon A, Kellman P, Hirsch GA, Aletras AH, Arai AE. Quantitative myocardial infarction on delayed enhancement MRI. Part I: animal validation of an automated feature analysis and combined thresholding infarct sizing algorithm. *J Magn Reson Imaging* 2006;23:298–308.
36. Hsu LY, Ingkanisorn WP, Kellman P, Aletras AH, Arai AE. Quantitative myocardial infarction on delayed enhancement MRI. Part II: clinical application of an automated feature analysis and combined thresholding infarct sizing algorithm. *J Magn Reson Imaging* 2006;23:309–14.
37. Kim RJ, Wu E, Rafael A, et al. The use of contrast-enhanced magnetic resonance imaging to identify reversible myocardial dysfunction. *N Engl J Med* 2000;343:1445–53.
38. Knuesel PR, Nanz D, Wyss C, et al. Characterization of dysfunctional myocardium by positron emission tomography and magnetic resonance: relation to functional outcome after revascularization. *Circulation* 2003;108:1095–100.
39. Kistler PM, Ho SY, Rajappan K, et al. Electrophysiologic and anatomic characterization of sites resistant to electrical isolation during circumferential pulmonary vein ablation for atrial fibrillation: a prospective study. *J Cardiovasc Electrophysiol* 2007;18:1282–8.
40. Verma A, Kilicaslan F, Pisano E, et al. Response of atrial fibrillation to pulmonary vein antrum isolation is directly related to resumption and delay of pulmonary vein conduction. *Circulation* 2005;112:627–35.
41. Peters DC, Wylie JV, Hauser TH, et al. Abstract 3371: Recurrence of atrial fibrillation following RF ablation correlates with the extent of post-procedural left atrial scarring on delayed-enhancement CMR. *Circulation* 2007;116:II760–1.
42. Ouyang F, Antz M, Ernst S, et al. Recovered pulmonary vein conduction as a dominant factor for recurrent atrial tachyarrhythmias after complete circular isolation of the pulmonary veins: lessons from double Lasso technique. *Circulation* 2005;111:127–35.
43. Gerstenfeld EP, Dixit S, Callans D, et al. Utility of exit block for identifying electrical isolation of the pulmonary veins. *J Cardiovasc Electrophysiol* 2002;13:971–9.
44. Ouyang F, Ernst S, Chun J, et al. Electrophysiological findings during ablation of persistent atrial fibrillation with electroanatomic mapping and double Lasso catheter technique. *Circulation* 2005;112:3038–48.

Key Words: delayed enhancement magnetic resonance imaging ■ atrial fibrillation ■ image processing.